

**$L_{2,3}$  threshold spectra of doped silicon and silicon compounds**

Frederick C. Brown,\* R. Z. Bachrach, and M. Skibowski†

*Xerox Palo Alto Research Center, Palo Alto, California 94304**and Materials Research Laboratory,‡ University of Illinois, Urbana, Illinois 61801*

(Received 3 December 1976)

Optical absorption in the neighborhood of the Si  $L_{2,3}$  edge ( $\sim 100$  eV) has been measured with high resolution in Si crystals with free-carrier concentration ranging from  $\sim 10^{14}$  to  $10^{20}$   $\text{cm}^{-3}$ , as well as in amorphous samples of Si,  $\text{SiO}_2$ , and  $\text{Si}_3\text{N}_4$ . In all crystalline samples a steep steplike threshold is observed, whose shape and height are insensitive to free-carrier concentration across the insulator-metal transition and in the whole range explored in the present investigation. A slightly different edge line shape is observed in amorphous Si films. Sharp threshold spikes are also present in amorphous  $\text{SiO}_2$  and  $\text{Si}_3\text{N}_4$ . These effects reflect a more localized final state. The results for crystalline Si are briefly discussed in terms of the similarity of the excess electronic charge distribution around the deep hole throughout the range of free-carrier densities investigated.

**I. INTRODUCTION**

The nature of the final state in x-ray transitions from core levels in a solid has long been a subject of considerable interest. Questions arise as to a correct description of the final-state wave function.<sup>1</sup> Clearly the hole in the inner shell is highly localized, but is the excited-electron wave function local like a deep impurity state or more extended as for a shallow donor? What happens to the final state when free carriers are present as in a heavily doped semiconductor? Are the transition matrix elements modified in the many-electron case so that threshold effects occur as for metals? We have attempted a direct experimental investigation of some of these matters.

In this paper we present new high-resolution data on the silicon  $L$  edge for silicon crystals containing various concentrations of electrons and holes.<sup>2</sup> The specific conductivity of each sample was carefully measured, and one  $n$ -type crystal contained a carrier density approaching  $10^{20}$   $\text{cm}^{-3}$ . Possible effects due to carrier screening of the electron-hole Coulomb interaction were sought in the threshold spectra. The results are discussed in the light of present understanding and directions for future investigation are indicated.

The silicon  $L_{2,3}$  threshold is well suited for detailed optical-absorption measurements. Although it lies at 100 eV, a difficult region as far as laboratory sources are concerned, this region is fully accessible with synchrotron radiation sources.<sup>3-5</sup> The  $L$  absorption overlies a relatively weak continuum due to outer-shell interband transitions and is therefore well resolved. The lifetime of a hole in the  $2p^6$  shell is relatively long corresponding to a Lorentzian linewidth  $\Gamma \sim 0.1$  eV caused primarily by Auger processes which fill the inner-shell hole.

The  $L$  edge of pure crystalline and amorphous

silicon was observed by Gähwiller, Rustgi, and Brown<sup>3,4</sup> using synchrotron radiation from the small electron storage ring at Stoughton, Wisc. Results for a thin film are shown in Fig. 1(a) where the upper curve shows the observed absorption coefficient for polycrystalline silicon and the lower curve Fig. 1(b) a similar scan for a thin amorphous silicon film. There are similarities in the two

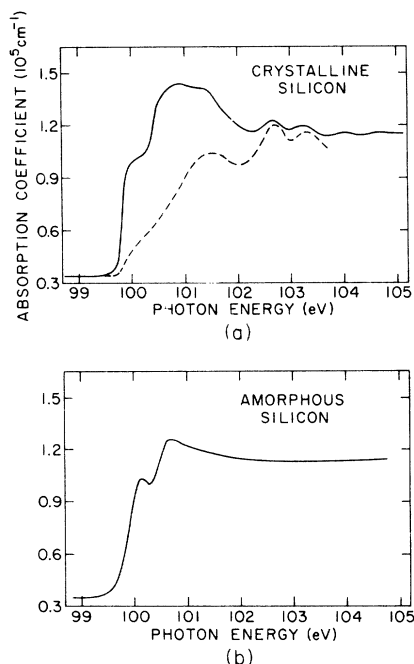


FIG. 1. Absorption coefficient vs photon energy at the silicon  $L_{2,3}$  threshold. (a) The observed spectrum for a crystalline sample. The dashed line shows the theoretical joint density of states for the  $2p^6$  core to  $\Delta_1$  band transition taking into account the 0.61-eV spin-orbit splitting of the core levels. (b) The observed  $L_{2,3}$  spectrum for an amorphous silicon film.

spectra but notice that the edge of the amorphous spectrum rises less rapidly to a kind of peak. The crystal spectrum contains more structure above threshold indicating that the transition definitely depends upon details of the final-state wave function and the presence of long-range order. In these scans the instrument resolution was about 0.02 eV, somewhat less than the rise in absorption at 99.8 eV corresponding to excitation of an electron from the  $2p$  inner shell to a final state associated with the  $\Delta_1$  minimum of the conduction band. Two thresholds are seen separated by  $0.61 \pm 0.02$  eV, the spin-orbit splitting of the  $j = \frac{3}{2}$ ,  $j = \frac{1}{2}$  inner-shell hole. The observed weight of these two states is found to be close to the expected 2:1 statistical weight of the initial core states.

A central feature of Fig. 1(a) is that the edge rises steeply at threshold, much faster than the conduction-band density of states shown by the dashed line in Fig. 1(a). Altarelli and Dexter<sup>6</sup> pointed out that this was evidence for important excitonic effects in core-electron transitions to the conduction band. These workers adapted the Elliot<sup>7</sup> effective-mass theory to the case of a localized core hole and a diffuse ( $\sim 20$  Å radius) conduction electron. It should be emphasized that in this theory enhancement arises through changes in the exciton envelope function  $|F_E(0)|^2$  and these affect the continuum absorption for many exciton rydbergs above threshold. It was assumed that exciton lines are not resolved because of a broadening  $\Gamma \approx 0.1$  eV much greater than the exciton rydberg,  $\sim 0.04$  eV. The calculated line shape was found to be in good agreement with experiment. On the other hand, the absolute value of the measured absorption was found to be about ten times larger than the effective-mass value. Reasonable agreement between theory and experiment for the absorption-edge strength was obtained by introducing a central-cell correction rather like that used in the phosphorous-donor-impurity problem. Thus in the theory of Altarelli and Dexter it was necessary to depart from a simple effective-mass exciton theory, but the excited electron is still in a rather large orbit, about 40 Å in diameter, with a charge density which is spread out in the crystal like that for a shallow donor impurity at low temperature.

Figure 2 shows the  $L$  absorption of silicon over an extended range of photon energies. Crystalline silicon is shown in the upper part of the figure without resolving the details of Fig. 1 near threshold. Notice the  $L_1$  threshold at 150 eV superimposed upon the decreasing portion of a broad " $p$  to  $d$ " maximum due to matrix-element effects and the nature of the continuum wave function. The weak secondary maximum at 168 eV is unexplained and may be part of the so-called extended x-ray

absorption fine structure for silicon. The effective number of electrons which contribute to the absorption is shown by the dashed line.<sup>3</sup> Less than 0.2 of the six  $2p$  core electrons contribute within the first 10 V of threshold.

For comparison we have reproduced the silicon  $L$  spectrum for silane gas<sup>8</sup> in the lower part of Fig. 2. Again the  $L_1$  edge and a broad  $p$  to  $d$  maximum is evident, however the details near threshold are quite different as shown in the inset. Here the strong band at 103 eV is probably to be associated with transitions to valence-like antibonding molecular orbitals  $\sigma$ . These are followed by Rydberg states beginning at 105 eV and terminating at about 107.5 eV.<sup>9</sup> Thus the binding energy of the Rydberg states is of the order of 2.5 eV and of the  $\sigma$  states about 4.5 eV much greater than the electron-hole binding in solid silicon. This is reflected in the strong threshold spike for the gas [Fig. 2(b)] as compared to weaker enhancement for the solid [Fig. 2(a)]. There is more overlap of the excited-electron wave function with the compact  $2p^6$  core in the silicon hydride case.

We take up the  $L$  edge for doped silicon in Sec.

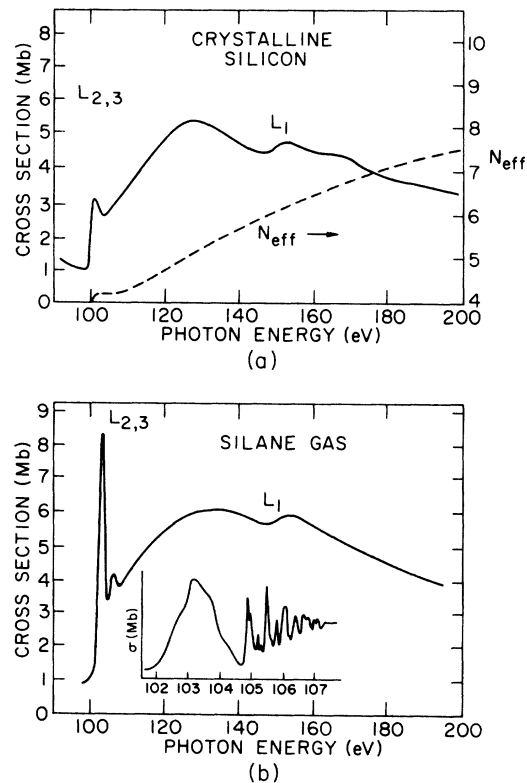


FIG. 2. (a)  $L$ -absorption cross section (Mb per atom) of solid silicon over a 100-eV energy range.  $N_{\text{eff}}$  is shown by the dashed curve and the scale on the right-hand side. (b) The absorption cross section for silane gas over a wide energy range.

II. Sample preparation and measurement techniques are described followed by typical threshold spectra. A possible interpretation of the results on doped silicon is given in Sec. III. Finally, new soft-x-ray data on silicon dioxide and silicon nitride are given in Sec. IV.

## II. EXPERIMENTAL METHODS AND RESULTS ON DOPED SILICON

Commercially grown doped silicon crystals were used. The crystals were sliced, mechanically polished, and then chemically polished to approximately 12  $\mu$  thickness. They were masked with epoxy except for a window area about 2 mm in diameter. Plasma etching was then used to reduce the thickness to 1  $\mu$ . Further reduction was accomplished with argon ion milling of the self-supporting window monitored by observing the transmitted light. Final window thicknesses were of the order of 1000–2000  $\text{\AA}$ . The carrier concentrations in each crystal were determined by measuring the electrical resistivity at room temperature using a commercial four-point probe. Characteristics of the nine crystals measured are listed in Table I. In a few cases free carrier absorption was observed by transmission through the etched and milled window. In at least one other case the far-infrared reflectivity was observed over a wide range of wavelengths. Figure 3 shows a reflectivity for sample No. 9, which was doped with phosphorus. The direct current measurements indicated a carrier concentration of  $9 \times 10^{19} \text{ cm}^{-3}$ . The Drude optical conductivity for a fit to Fig. 3 was in order-of-magnitude agreement with the low-frequency measurements. We believe that the thinning process does not appreciably compensate the samples.

Finally, a number of thin amorphous samples containing silicon were prepared by various techniques. Results for these will be discussed in Sec. IV. For example, amorphous Si films were made

TABLE I. Characteristics of silicon samples studied.

No.	Dopant and type of conductivity	Resistivity ( $\Omega \text{ cm}$ )	Carrier density ( $\text{cm}^{-3}$ )
1	<i>n</i> type	110	$10^{14}$
2	<i>P n</i> type	3	$1.5 \times 10^{15}$
3	<i>p</i> type	1.0	$1.5 \times 10^{16}$
4	<i>P n</i> type	0.9	$6 \times 10^{15}$
5	<i>P n</i> type	0.02	$2 \times 10^{18}$
6	<i>P n</i> type	0.015	$3 \times 10^{18}$
7	<i>Sb n</i> type	0.015	$3 \times 10^{18}$
8	<i>Sb n</i> type	0.007	$8 \times 10^{18}$
9	<i>P n</i> type	0.000 74	$9 \times 10^{19}$

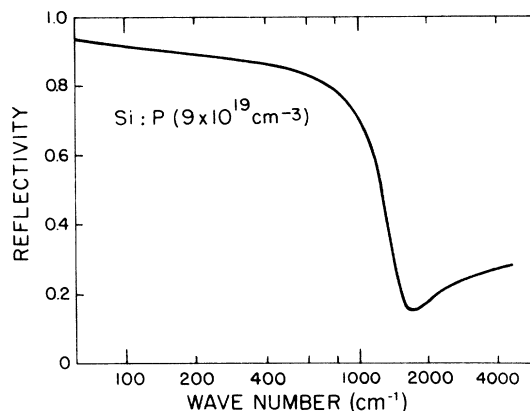


FIG. 3. Far-infrared reflectivity for a polished surface of silicon sample No. 9 containing  $9 \times 10^{19}$  phosphorus donors/ $\text{cm}^3$ .

by plasma decomposition of silane. These films were floated off the substrate and mounted on transmission electron microscope screens.  $\text{Si}_3\text{N}_4$  and  $\text{SiO}_2$  were made by gas-phase reaction of silane with ammonia or  $\text{CO}_2$  onto GaAs. The films were removed by dissolving the GaAs.

Absorption spectra were measured at room temperature using the soft-x-ray  $2^\circ$  grazing incidence monochromator at the Stanford Synchrotron Radiation Project.<sup>5</sup> The samples were placed on a sample slide in ultrahigh vacuum about 2 cm from the exit slit of the monochromator so that a highly focussed beam was transmitted through a part of the 2-mm window area. See Fig. 4. A spiraltron

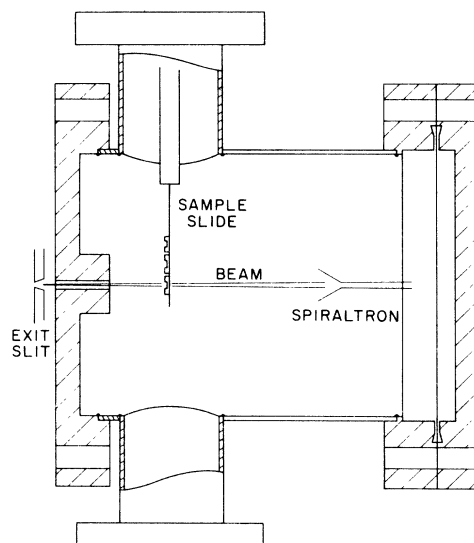


FIG. 4. Sample and detector chamber on a 6-in. ultra-high vacuum flange just beyond the exist slit of the 2-m grazing incident monochromator at the Stanford Synchrotron Radiation Project.

channel multiplier was used to detect single photons in a high-speed counting mode with a slow scan. The monochromator bandwidth at 100 eV is approximately 0.08 eV in first order. By observing the silicon edge in third order, a resolution of 0.025 eV was available.

Figure 5(a) shows the absorption edge for crystalline silicon for a lightly doped and a very heavily doped sample containing  $10^{14}$  and  $9 \times 10^{19}$  carriers per  $\text{cm}^3$ , respectively. The details of these spectra agree well with those obtained previously for undoped silicon. Several aspects of the curves are important; the strength, position, and steepness of the absorption, and the occurrence of edge structure which can be associated with the band density of states (see Fig. 1). These various features have been discussed elsewhere.<sup>4</sup> What is remarkable is that the curve for the heavily doped crystal is almost identical to that for the lightly doped crystal. Certainly the enhancement at threshold relative to the structure one or two volts above threshold is little affected by the presence of carriers. There is a slight rounding of the very first maximum of the highly doped crystal approximately 0.2 eV above threshold. This is shown by the energy derivative of absorption Fig. 5(b), and it may indicate

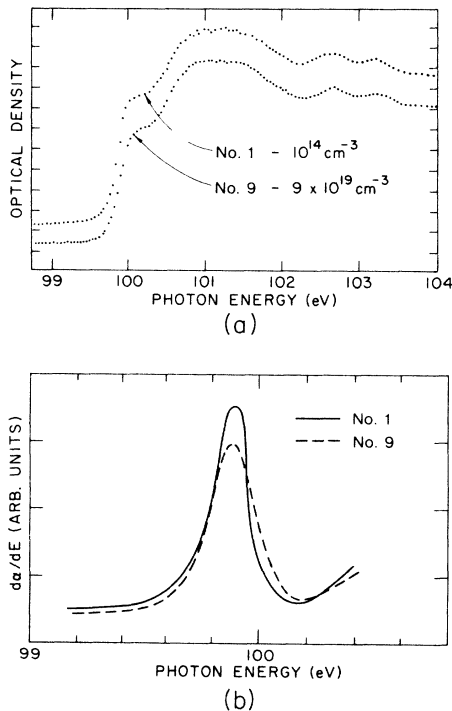


FIG. 5. (a) Data showing the absorption edge of crystalline silicon sample No. 1 ( $\sim 10^{14}$  carriers  $\text{cm}^3$ ) and sample No. 9 ( $9 \times 10^{19}$  electrons/ $\text{cm}^3$ ). (b) Derivative of absorption edges for samples No. 1 and 9 on a greatly expanded scale.

the onset of carrier effects at  $10^{20} \text{ cm}^{-3}$ . Other samples listed in Table I yielded spectra which could not be distinguished from an intrinsic crystal. In this regard our results do not agree with the recent suggestion that moderate carrier concentrations affect the shape of the silicon  $L$  edge.<sup>10</sup>

An estimate of the Fermi level and band population effects in a crystal containing  $n_0$  electrons/ $\text{cm}^3$  can be made in the usual way.<sup>11</sup> For this purpose we use the expression

$$n_0 = S(1/2\pi^2)(2mkT/\hbar^2)^{3/2} \times (\mu_L \mu_T)^{1/2} F_{1/2}(E_F/kT), \quad (1)$$

where  $S=6$ , the number of conduction-band minima lying along the  $\langle 100 \rangle$  directions,  $F_{1/2}(E_F/kT)$  is the Fermi-Dirac integral, and  $\mu = m_c^*/m$ , the ratio of conduction-band mass to free-electron mass. An appropriately averaged single valley mass  $m_c^{*3} = m_L^* m_T^{*2}$  is used to account for anisotropy ( $\mu_L=0.98$ ,  $\mu_T=0.19$ ). For  $n_0=10^{20} \text{ cm}^{-3}$  the tables of Fermi integrals<sup>12</sup> show that  $E_F=0.072 \text{ eV}$ . Alternate treatments including the effect of non-parabolicity result in only a slightly different Fermi level. Basically the Burstein-Moss shift in silicon is not very large, compared to InSb, for example. This is mainly a consequence of fairly large effective masses. The data of Fig. 5 do not indicate much, if any, resolvable shift with doping and there is little or no weakening of the enhancement above threshold. We turn to an interpretation of these results in Sec. III.

### III. INTERPRETATION OF RESULTS ON DOPED SILICON

Combescot and Nozières<sup>13</sup> discuss the many-electron aspect of the final state in an excited semiconductor across the metal-insulator transition. Their results however are not really relevant in the present case because their schematic model focusses on details of line shape which are obscured by lifetime effects in the real case. Before discussing the high carrier density limit let us consider an admittedly oversimplified screened exciton model for the low-density case, e.g., one that makes use of a modified Coulomb potential. For example, one suspects that the following screened potential might be appropriate in the spirit of a simplest effective-mass theory:

$$U = (e^2/\epsilon r)e^{-k_s r}, \quad (2)$$

where  $\epsilon$  is an effective dielectric constant ( $\sim 11.4$  for Si) and a classical inverse screening length  $k_s$  is given by

$$k_s = (4\pi n e^2/\epsilon kT)^{1/2}. \quad (3)$$

At room temperature  $T$  with a carrier density  $n \approx 10^{18} \text{ cm}^{-3}$  it turns out that  $1/k_s \approx 40 \text{ \AA}$ . Equation

(2) would be somewhat different in the case of high degeneracy but recent experimental evidence<sup>14</sup> indicates that the transition to metallic state does not occur until about  $5 \times 10^{18} \text{ cm}^{-3}$ .

A simple model calculation for the screened exciton absorption has been reported by Dow.<sup>15</sup> This is a static-screening theory in which an effective-mass Schrödinger equation is solved with a potential which closely approximates Eq. (2) and in which energy levels and transition probabilities are computed ignoring the Pauli antisymmetry requirement in the initial and final states. Results are shown in Fig. 6 for various values of  $k_s a$ , where  $k_s$  is a screening wave vector and  $a = \hbar^2 \epsilon / m e^2$ . Notice that in the extreme metallic limit  $k_s a \rightarrow \infty$  one has a square-root energy dependence above threshold as in an  $M_0$  band-to-band transition. In the insulator limit  $k_s a \rightarrow 0$ , an exciton line develops, and there is appreciable enhancement for several rydbergs above threshold, as in the Elliott theory.<sup>7</sup> In between these two-limiting values a sharp spike develops which would not be observable if instrument resolution is too low or if there is too much lifetime broadening.

The naive picture according to which the conduc-

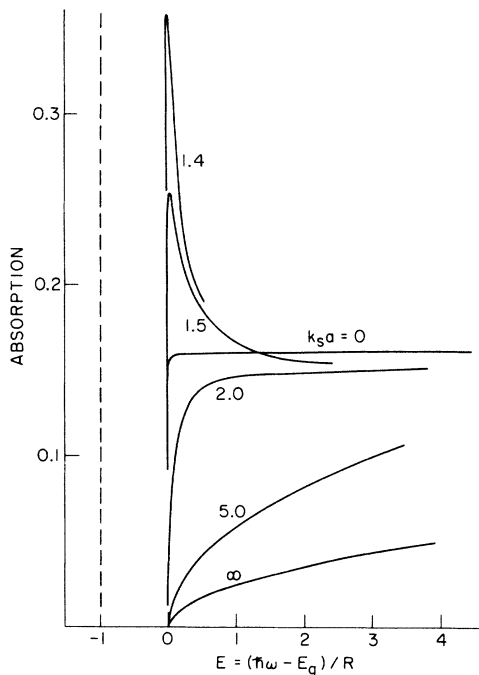


FIG. 6. Showing schematically the behavior expected for a simple theory at the exciton series limit as the screening increases from zero  $k_s a = 0$  to high values  $k_s a \geq 5.0$ . From J. D. Dow, Ref. 14. The Fermi energy  $E_F$  (not shown in this figure) displaces to the right-hand side with increasing carrier screening. States below  $E_F$  would not be accessible for optical transitions from the core.

tion electrons screen the electron-hole interaction, resulting in a delocalized, plane-wave-like final state, and consequently in a suppression of the excitonic enhancement at threshold, is to be rejected after detailed consideration of two aspects of the problem: (a) the screening *charge distribution* around a positive charge in an electron gas; (b) the amplitude for optical transitions in a many-electron system.

First let us consider point (a). When the conduction electrons are absent, an electron is ejected out of the core state and, in the final state corresponding to threshold absorption, is localized in a region of the order of the effective Bohr radius (assume, for the time being, infinite core lifetime). When  $N$  conduction electrons are present, the final state is the ground-state configuration of an  $N + 1$  electron system in the presence of an approximately pointlike, heavy positive charge. For the highest densities considered in this work,  $n \sim 10^{20} \text{ cm}^{-3}$ , this electron gas is characterized by an inverse Fermi momentum  $k_F^{-1}$  of the order of 12 Å (assuming six isotropic valleys), which is comparable to the effective Bohr radius of a phosphorus donor in Si, 20 Å.

Recent calculations<sup>16-18</sup> of the polarization charge around a positive impurity, which have succeeded in including the strong deviations from linear response (thus correcting previous underestimates of the charge density at the origin) show that for densities up to about one electron per Bohr sphere ( $k_s a \geq 2$ ) the polarization charge distribution is very similar to that of a hydrogenic atom, and for higher densities it becomes even more localized. The maximum densities of the present experiment on doped silicon would correspond to  $k_s a \sim 1$ , if the scaling with  $\epsilon$  and  $m^*$  is taken at face value.

Therefore, in both cases of insulating and metallic samples, threshold absorption corresponds to a final state in which one excess electronic charge is localized within an effective Bohr radius from the hole. Central-cell effects are also expected to be the same in both cases, due to their highly localized nature.

The difference between the two cases, of course, appears in the behavior at larger distances (exponential decay of the bound state versus Friedel oscillations of the metallic system), and more importantly in the fact that in the metallic state the charge pileup does not result from the presence of one electron in a bound state, but from the interference of the slight distortions of all the free-electron wave functions in the presence of the hole. We are therefore led to the problem of evaluating the transition probability to this final state of the many-body system, point (b) above.

This problem of estimating the transition rate is

the same as that faced in the theory of x-ray edges in metals. In its most convenient formulation the calculation makes use of Hartree-Fock determinantal wave functions to describe initial and final states. The transition probability results from the interference of "direct" and "replacement" transition amplitudes as explained by Friedel.<sup>19</sup> This interference phenomenon is the same giving rise to the edge singularities. We are not interested in these details of the line shape, however, as they take place over an energy range of order  $E_F$ , and are therefore washed out by the lifetime broadening of the hole. What we are basically interested in is the height of the absorption step at threshold. (An analysis of the line shape across the insulator-metal transition is attempted by Combescot and Nozières in Ref. 13.)

We believe that the invariance of the absorption step across the carrier density region explored here is a reflection of the substantial invariance of the localization of the excess electronic charge. This can be shown exactly in a simplified case in which we take the hole to be spherically symmetric, assume nonvanishing phase shifts for  $s$  waves only, and neglect the electron spin. This is equivalent to assuming very large Coulomb repulsion between opposite spin electrons in the neighborhood of the core hole<sup>13</sup>; therefore, we imply that the screening cloud is made out of electrons with a definite spin orientation. (This is certainly the case for the low-density limit when the electron bound in an exciton state has a definite spin. Admittedly it is an unproven assumption at higher densities.)

With these simplifying assumptions, the Friedel sum rule shows that the phase shift for the only relevant channel varies between 0 and  $\pi$  when the energy varies between 0 (the bottom of the band) and  $E_F$ . In this case it was shown by Flynn<sup>20</sup> that a unitary transformation takes the final-state determinant of perturbed plane waves into one composed of a localized one-electron state plus a set of initial unperturbed plane waves. One then obtains a line spectrum with strength very similar to that of the exciton line, because of the close similarity of the localized virtual state to the exciton state of the insulating limit, in the neighborhood of the core hole, as discussed above [point (a)]. In the general case of a contribution of various channels to the phase shifts and therefore to the displaced charge, the line spectrum will be broadened by the creation of quasiparticles, but this should redistribute the oscillator strength over an energy of the order of  $E_F$  and therefore, because of the hole lifetime, should not be observable in this experiment.

We thus come to the point of view that the final

state in the doped crystals is a many-electron state with a charge distribution rather like that for an exciton in intrinsic silicon. This distribution is more localized than  $40 \text{ \AA}$ , however, since a strong central cell correction is required.<sup>6</sup> The exciton binding energy cannot be much more than 0.1 eV or so, otherwise a line would be observable at threshold broadened by the core hole lifetime. In fact, a kind of peak does appear at threshold in the amorphous silicon samples. A search for electroreflectance signals at the silicon  $L_{2,3}$  edge has recently been carried out.<sup>21</sup> Although the reflectivity  $R$  was observed with high resolution, no modulation structures  $\Delta R/R$  was observed for Schottky barrier fields as high as  $3 \times 10^5 \text{ V/cm}$ . Everything considered, this is still consistent with the above doping results and interpretation.

Conceivably some information about exciton binding energy could be obtained from photoemission experiments on silicon. These should be carried out using photons of sufficient energy to excite from the  $L$  core as well as from the valence band. It can be argued that the difference between the highest valence-band energy and the  $L_3$  core level plus the band gap equals the absorption threshold energy, exclusive of exciton binding energy. On the other hand, it is difficult to make this comparison with an accuracy much better than 0.5 eV.<sup>21,22</sup> For one thing band bending at the surface can occur; also additivity has not been demonstrated to this precision.

In some respects screenings of the soft-x-ray excitation of silicon closely resembles the phosphorus donor electron system. A shift is seen in the <sup>31</sup>P nuclear magnetic resonance frequency with increasing donor concentration into the metallic range.<sup>14</sup> The shift can be related to the probability amplitude of conduction electrons at the donor nucleus, but the spin component of the static magnetic susceptibility  $\chi_s$  is involved. Changes in  $\chi_s$  may accompany the NMR shift through the non-metal-metal transition, therefore it is difficult to be certain about the electron distribution whose changes may be too small to observe in soft-x-ray absorption. More important, the NMR experiments indicate that conduction electrons are fairly strongly concentrated on the donor nuclear site even in the metallic concentration range. We believe that this electron distribution more or less resembles the probability amplitude in the insulating or low-concentration case.

#### IV. SPECTRA FOR SOME AMORPHOUS SILICON COMPOUNDS

A number of amorphous silicon samples, and compounds containing silicon, were prepared by

gas-phase reaction of silane. Amorphous silicon films prepared by plasma decomposition of silane yielded spectra very close earlier work<sup>3,4</sup> where the amorphous material was made by vacuum evaporation [see Fig. 1(b)]. The threshold of the  $L_3$  absorption in amorphous silicon occurs about  $0.15 \pm 0.05$  eV higher energy than in crystalline silicon. The threshold is also slightly less steep.

On the other hand, the silicon  $L$  threshold for an amorphous  $\text{SiO}_2$  film is shifted to  $106 \pm 0.5$  eV presumably because of a transfer of electronic charge to the more electronegative oxygen. Figure 7(a) shows the spectrum of amorphous  $\text{SiO}_2$  over a wide energy range. The  $p$  to  $d$  maximum and  $L_1$  edge are clearly visible but the structure is quite different than for amorphous silicon. One is tempted to explain the two peaks at threshold in terms of excited molecular orbitals as for the molecular gases. The remaining features probably are extended-fine-structure characteristic of the local order of  $\text{SiO}_2$ . Our results are in agreement with Lukirskii and co-workers<sup>23</sup> who, on this extended scale, obtained similar silicon  $L$  spectra in both crystalline and amorphous  $\text{SiO}_2$ . These workers also measured the oxygen  $K$ -shell spectrum which begins at about 535 eV.

Figure 7(a) also shows the silicon  $L$  absorption

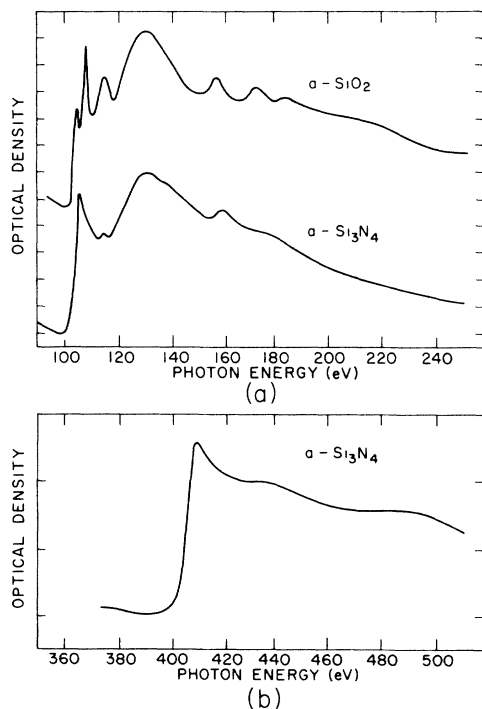


FIG. 7. (a) Silicon  $L_{2,3}$  absorption over a wide energy range for amorphous chemical-vapor-deposition films of  $\text{SiO}_2$  and  $\text{Si}_3\text{N}_4$  (optical density scale has been shifted vertically for clarity). (b) The nitrogen  $K$  edge above 400 eV for an amorphous  $\text{Si}_3\text{N}_4$  film.

for a thin amorphous film of  $\text{Si}_3\text{N}_4$ . Here the threshold and extended structure is much closer to that of amorphous silicon, however the edge is broadened and chemically shifted to  $100.2 \pm 0.2$  eV. The spectrum is quite different than for  $\text{SiO}_2$ , no doubt due to different short-range order. Finally Fig. 7(b) shows the  $K$ -shell threshold for nitrogen recorded with about 2-eV resolution at 400 eV. Notice that a peak still appears at threshold but that the  $p$  to  $d$  maximum is absent, as it should be.

As a general conclusion for the silicon  $L$  absorption, we find that both the extended and threshold structure is sensitive to environment, especially the neighboring atoms and their arrangement. The near threshold structure (within 3–4 eV of onset) is somewhat broadened and featureless in amorphous samples compared to well-characterized crystalline samples which show vestiges of the band density of states reflecting long-range order. Electron-hole interaction or excitonic enhancement does appear to be important within a few electron volts of threshold in both cases. In high-resistivity crystalline silicon the wave function of the electron excited at threshold does appear to be spread out over many neighbors (although it is more compact in  $\text{SiH}_4$  gas and possibly in open structures like  $\text{SiO}_2$ ). In doped crystals the spectrum cannot be altered appreciably through electron screening even for carrier concentrations as high as  $10^{20} \text{ cm}^{-3}$ . It appears that charge density in the many-electron final state is very similar to that for the excitons in an insulator, at least where this charge overlaps the localized core hole. On the other hand, interesting effects may appear just above the carrier densities studied in this work as the Fermi energy substantially exceeds the linewidth associated with lifetime broadening. The onset of these effects may have been seen in the present investigations.

It is difficult to grow and characterize homogeneous samples having carrier concentration greater than  $10^{20} \text{ cm}^{-3}$  as studied in this work. It should be possible to achieve another factor of 10 near the surface of a crystal either by diffraction or ion implantation. In such a case the  $L_{2,3}$  spectrum might be studied by means of total yield spectroscopy.<sup>24</sup>

#### ACKNOWLEDGMENTS

The authors would like to express their appreciation to the Director and staff of the Stanford Synchrotron Radiation Project for their assistance during runs on the 4-deg beam line. This project is supported by NSF Grant No. DMR-73007692 A02 in cooperation with the U. S. Energy Research and Development Administration. We would also like

to thank A. Alimonda, T. Tramontana, D. Thornburg, and D. Scifres for their patience and assistance during preparation of our samples. The silicon crystals were obtained from various sources, and we would like to thank T. Castner, H. Fujita,

and S. Groninger for the uniform heavily doped samples. Helpful comments on band population effects were made by H. Bottke. Finally, stimulating conversations with M. Altarelli, J. D. Dow, and C. P. Flynn are gratefully acknowledged.

\*Dept. of Physics and Materials Research Laboratory, Univ. of Illinois.

†University of Illinois. Present address: Institut für Experimentalphysik, University of Kiel, Germany.

‡Supported in part by NSF Grant No. DMR-76-01058.

<sup>1</sup>F. Bassani, *J. Phys. (Paris) Suppl.* **33**, C 3 (1972).

<sup>2</sup>Preliminary aspects of this work were presented at the March 1975 American Physical Society Meeting, Denver, Colo. by R. Z. Bachrach, F. C. Brown, and M. Skibowski, *Bull. Am. Phys. Soc.* **20**, 488 (1975).

<sup>3</sup>C. Gähwiller and F. C. Brown, in *Proceedings of the Tenth International Conference on the Physics of Semiconductors*, Cambridge, Mass., 1970, edited by S. P. Keller, J. C. Hensel, and F. Stern, CONF 700801 (U.S. Atomic Energy Commission, Division Technical Information, Springfield, Va., 1970), p. 213.

<sup>4</sup>F. C. Brown and O. P. Rustgi, *Phys. Rev. Lett.* **28**, 497 (1972).

<sup>5</sup>F. C. Brown, R. Z. Bachrach, S. B. M. Hagstrom, N. Lien, and C. H. Pruet, in *Vacuum Ultraviolet Radiation Physics*, edited by E. Koch, R. Haensel, and C. Kunz (Pergamon, New York, 1974).

<sup>6</sup>M. Altarelli and D. L. Dexter, *Phys. Rev. Lett.* **29**, 1100 (1972).

<sup>7</sup>R. J. Elliott, *Phys. Rev.* **108**, 1384 (1957).

<sup>8</sup>W. Hayes and F. C. Brown, *Phys. Rev. A* **6**, 21 (1972).

<sup>9</sup>M. Robin, *Chem. Phys. Lett.* **31**, 140 (1975).

<sup>10</sup>H. Fujita and Y. Iguchi, *J. Appl. Phys. Jpn.* **14**, 220 (1975).

<sup>11</sup>H. Bottke and D. L. Johnson, *Phys. Rev. B* **11**, 2969 (1975).

<sup>12</sup>A. C. Beer *et al.*, *Helv. Acta. Phys.* **28**, 534 (1955).

<sup>13</sup>M. Combescot and P. Nozières, *J. Phys. (Paris)* **32**, 913 (1971; see also J. Gavoret, P. Nozières, B. Roulet, and M. Combescot, *ibid.* **30**, 987 (1969)).

<sup>14</sup>W. Sasaki, S. Ikehata, and S. Kobayashi, *J. Phys. Soc. Jpn.* **36**, 1377 (1974); **39**, 1492 (1975).

<sup>15</sup>J. Dow, in *Proceedings of the Twelfth International Conference on Semiconductors, Stuttgart, 1972*, edited by M. H. Pilkuhn (Teubner, Stuttgart, 1974), p. 957.

<sup>16</sup>P. Bhattacharyya and K. S. Singwi, *Phys. Rev. Lett.* **29**, 22 (1972).

<sup>17</sup>Z. D. Popovic, M. J. Stott, J. P. Carbotte, and G. R. Piercy, *Phys. Rev. B* **13**, 590 (1976).

<sup>18</sup>C. O. Almbladh, U. Von Barth, Z. D. Popovic, and M. I. Stott, *Phys. Rev. B* **14**, 2250 (1976).

<sup>19</sup>J. Friedel, *Comments Solid State Phys.* **2**, 40 (1969).

<sup>20</sup>C. P. Flynn, *Phys. Rev. B* (to be published).

<sup>21</sup>R. S. Bauer, R. Z. Bachrach, D. E. Aspnes, and J. C. McMenamin, *Nuovo Cimento* (to be published).

<sup>22</sup>G. Margaritondo and J. Rowe, *Phys. Lett. A* **59**, 464 (1977).

<sup>23</sup>O. A. Ershov and A. P. Lukirskii, *Fiz. Tverd. Tela* **8**, 2137 (1966) [*Sov. Phys.-Solid State* **8**, 1699 (1967)]; O. A. Ershov, D. A. Goganov, and A. P. Lukirskii, *ibid.* **7**, 1903 (1966).

<sup>24</sup>W. Gudat and C. Kunz, *Phys. Rev. Lett.* **29**, 169 (1972).